

Exploring the Structural Diversity of DNA Bottlebrush Polymers Using an Oligonucleotide Macromonomer Approach

Hao Lu,[§] Jiansong Cai,[§] Yang Fang, Mengqi Ren, Xuyu Tan, Fei Jia, Dali Wang, and Ke Zhang*



Cite This: *Macromolecules* 2022, 55, 2235–2242



Read Online

ACCESS |



Metrics & More

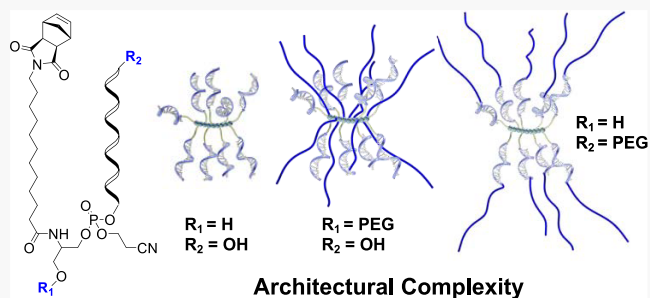


Article Recommendations



Supporting Information

ABSTRACT: Herein, we demonstrate that macromonomers consisting of organics-soluble, chemically protected oligonucleotides (protDNA) and poly(ethylene glycol) (PEG) chains can be converted into bottlebrush polymers of distinct architectures via ring-opening metathesis polymerization. Using a custom norbornene-containing phosphoramidite, two types of macromonomers were obtained: a linear norbornene-protDNA-PEG structure and a Y-shaped structure where the polymerizable norbornene group is situated at the junction where protDNA and PEG meet. With this strategy, the PEG chains can be placed either near the backbone of the bottlebrush or on its periphery, and in principle anywhere between these two extremes by adjusting the norbornene location, which makes this strategy attractive for constructing architecturally sophisticated oligonucleotide-containing copolymers.



INTRODUCTION

Oligonucleotides hold tremendous potential in a variety of applications spanning therapeutics,^{1–4} diagnostics,^{5–8} biotechnology,^{9,10} and nanotechnology.^{11–14} In many of these applications, it is often necessary for oligonucleotides to be covalently attached to other chemical entities, for example to introduce additional functionalities^{15–17} or to modify intrinsic characteristics^{18,19} (e.g., poor enzymatic stability and low cellular uptake) of the oligonucleotide itself. Following the development of traditional linear oligonucleotide-ligand conjugates, more sophisticated architectures have recently been shown to provide interesting and often superior properties.²⁰ For example, the bottlebrush-type “poly(oligonucleotide)” structure exhibits improved resistance against nuclease degradation and enhanced cellular uptake compared with free oligonucleotides because of sterics and increased local salt concentration.^{21,22} In general, these multivalent polymers can be synthesized via two routes, (1) “graft onto”, that is, conjugating the oligonucleotide onto a presynthesized polymer backbone or (2) “graft through”, referring to the direct polymerization of a nucleic acid-based macromonomer. In the former strategy, the coupling efficiencies are often compromised by the strong electrostatic repulsion between the negatively charged oligonucleotide chains and the difficulty in finding a common solvent for both the oligonucleotide and the synthetic polymer.^{23,24} Thus, it is very difficult, if not impossible, to synthesize quantitatively derivatized, highly polyvalent poly(oligonucleotide)s by the graft-onto methodology.^{25–27} On the other hand, while the graft-through approach should in principle overcome incomplete grafting, it still faces monomer solubility issues in organic

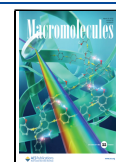
solvents because of the highly polar nature of the phosphate diester nucleic acid backbone,^{28,29} and the fact that many polymerization reactions are incompatible with nucleic acids because of nucleophilic, basic, coordination, and redox reactivities.^{30,31}

Prominent solutions to these problems include Gianneschi’s organic-phase polymerization of the noncharged oligonucleotide analogue, peptide nucleic acids,³² and Herrmann’s phase-transfer surfactant approach that enabled the polymerization of native oligonucleotides in dichloromethane (DCM).³³ More recently, O’Reilly et al. reported an aqueous copolymerization approach to synthesize DNA-containing bottlebrush polymers via direct graft-through ring-opening metathesis polymerization (ROMP).³⁴ We have previously reported a facile synthetic strategy to prepare bottlebrush-type poly(oligonucleotide)s using organic-soluble, temporarily protected oligonucleotide macromonomers.²² The protecting groups blocking the exocyclic amines of the nucleobases and the negative charge of the phosphate diester backbone were inherited from conventional solid-phase nucleic acid synthesis and retained using a nonprotecting cleavage condition. The resulting free sulfhydryl group on the oligonucleotide is then coupled to the polymerizable norbornene moiety via thiol-

Received: January 2, 2022

Revised: February 15, 2022

Published: March 1, 2022



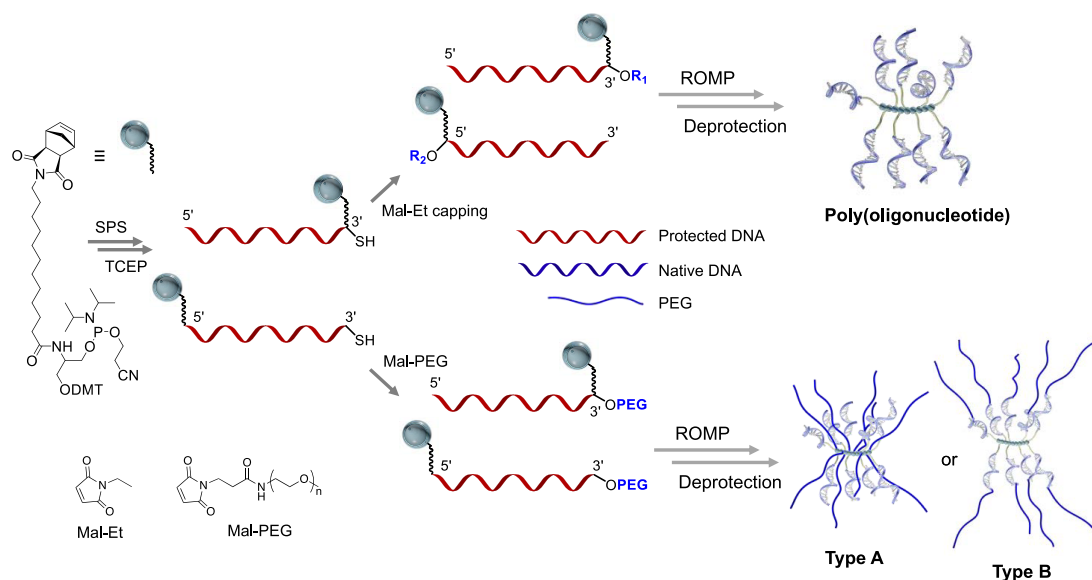
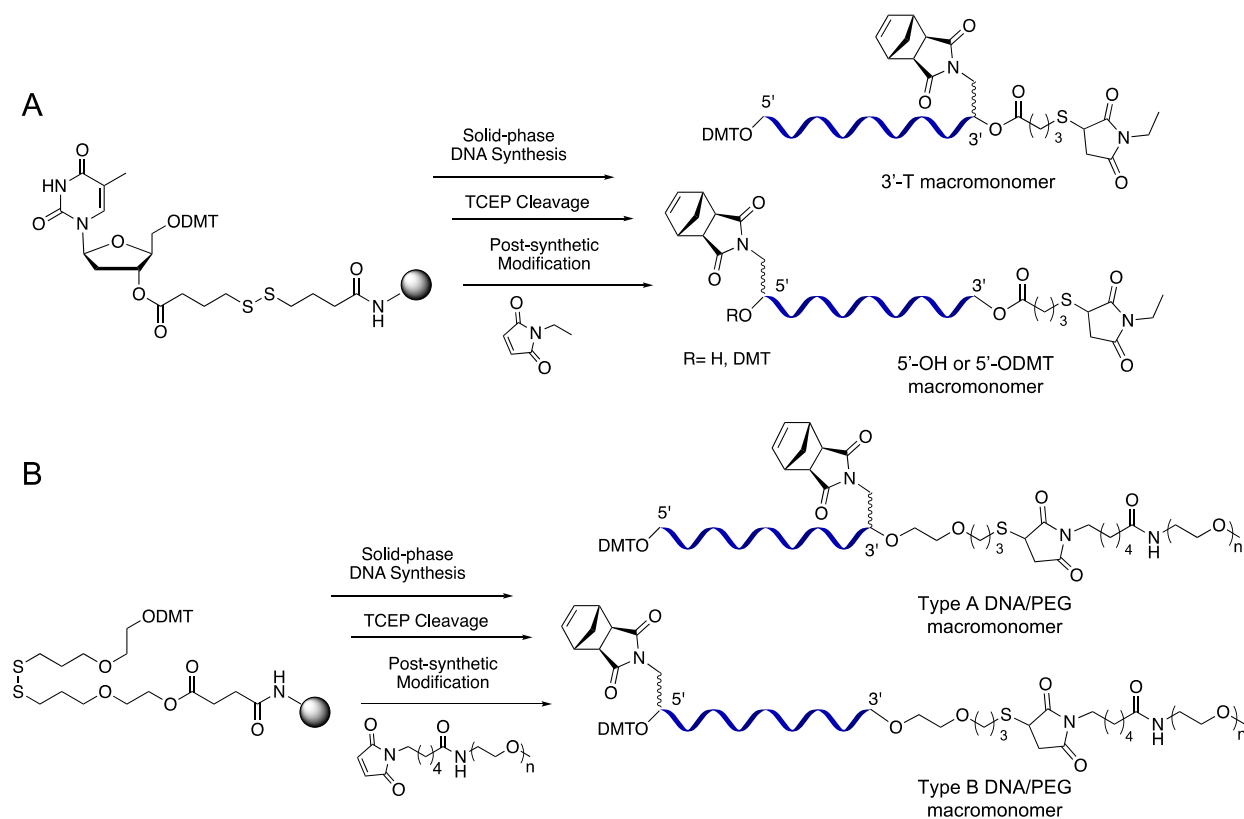


Figure 1. Schematic representation of macromonomer synthesis, norbornene/PEG location, and bottlebrush polymer synthesis. SPS: solid-phase synthesis.

Scheme 1. (A) Synthesis of protDNA with 5' or 3' Norbornene (3'-T, 5'-OH, and 5'-ODMT). (B) Synthesis of protDNA-b-PEG (Type A and Type B) Macromonomers



maleimide coupling. The oligonucleotide macromonomer can be polymerized in high yields via ROMP to give the bottlebrush precursor, which, upon mild deprotection, yields water-soluble poly(oligonucleotide)s.

In this study, we further explore the protected DNA (protDNA) system by developing a polymerizable norbornene phosphoramidite modifier.³⁵ Instead of coupling the norbornene functionality to the oligonucleotides at the 3', the

norbornene phosphoramidite can be directly used during solid-phase DNA synthesis for incorporation at any position within the DNA strand. The 3' terminal thiol group can either be used to conjugate with other moieties, such as poly(ethylene glycol) (PEG), resulting in diblock side chains in the final bottlebrush polymer, or be removed in a traceless manner if not needed or for later use (e.g., polymerase elongation). This strategy has led to two architecturally complex poly-

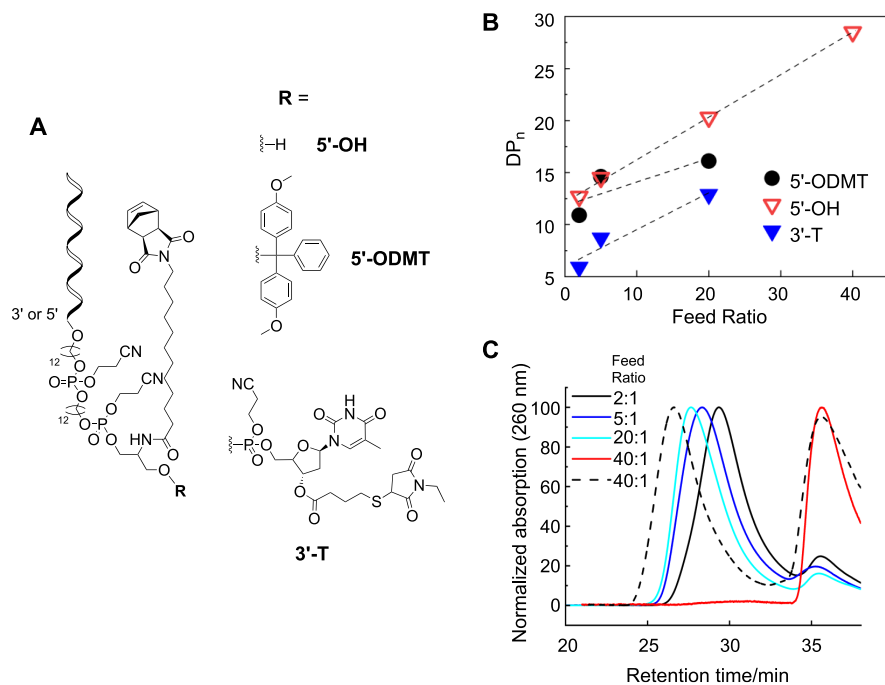


Figure 2. (A) ProtDNA macromonomer chemical structure (5'-OH, 5'-ODMT and 3'-T). Various neighboring groups surrounding the polymerizable norbornene group, including a free hydroxyl (5'-OH), 4,4'-dimethoxytrityl (5'-ODMT), and deoxythymidine (3'-T), are highlighted as they may interfere with ROMP. (B) Number-average degree of polymerization of the macromonomers as a function of monomer/initiator feed ratio (2, 5, 20, and 40). (C) Aqueous GPC of the 5'-ODMT and the 5'-OH (dashed line) macromonomers and corresponding bottlebrush polymers at indicated feed ratios. The results are for crude polymerization mixtures; the quantities of unreacted monomers were used to calculate reaction yields.

(oligonucleotide)-*co*-PEG polymers, with the PEG being attached either near the bottlebrush backbone or at the termini of the side chains (Figure 1). These materials, being compositionally similar and mainly differing in architecture, allow one to study the impact of polymer architecture on the properties of the grafted DNA. Overall, our approach greatly simplifies the synthesis of poly(oligonucleotide)s with complex architectures and paves the way for advanced functional studies and applications.

RESULTS AND DISCUSSION

Synthesis of Norbornene Phosphoramidite and the protDNA Macromonomer. The norbornene modifier is synthesized in high yield in four steps. *Cis*-5-norbornene-*exo*-2,3-dicarboxylic anhydride is first elongated by reaction with 12-aminododecanoic acid (Scheme S1). Then, the norbornene moiety (1) is conjugated to 2-amino-1,3-propanediol (serinol) by amidation. One of the serinol hydroxyl groups is then protected by a 4,4'-dimethoxytrityl (DMT) group, and the remaining one is transformed to a phosphoramidite by reacting with 2-cyanoethyl *N,N*-diisopropylchlorophosphoramidite. The isolated yield for the phosphoramidite (4) is 71%. The norbornene phosphoramidite dissolves readily in anhydrous acetonitrile and is fully compatible with automated oligonucleotide synthesis. To avoid unwanted iodination of the norbornene double bond during the oxidation step of the solid-phase DNA synthesis, a noniodine oxidizer (1*S*)-(+)-(10-camphorsulfonyl)-oxaziridine is selected. With 15 min coupling time, the conjugation efficiency is ~90% by trityl monitoring, which is typical of phosphoramidite modifiers.³⁵

To cleave the oligonucleotide from the solid support without inadvertent deprotection of the base-labile protecting groups

for purines and cytosine, a disulfide-linked controlled pore glass (CPG) is used as the support. Cleavage by tris(2-carboxyethyl)-phosphine (TCEP) under mildly acidic conditions allows for reductive strand release and generates a free sulfhydryl at the 3'. To avoid poisoning of the Grubbs catalyst by the sulfhydryl group during ROMP, the sulfhydryl is capped by a thiol-capping agent, *N*-ethylmaleimide (Mal-Et, Scheme S2). Additionally, a base-labile ester is used to link the CPG to thymidine, which is the first nucleotide (Scheme S1). During the final deprotection step postpolymerization, hydrolysis of the ester linkage removes the 3' sulfhydryl moiety, exposing a nonphosphorylated thymidine at the 3' of the oligonucleotide. This "traceless" design avoids the presence of a large number of free or capped sulfhydryl groups on the distal termini of the final bottlebrush polymer side chains, which may lead to aggregation or pose interference in biological applications. Using a 15-nucleotide antisense sequence against human HER2 mRNA as a model oligonucleotide, protDNA macromonomers with the norbornene group positioned at either 5' or 3' were prepared. After cleavage and sulfhydryl-capping, the macromonomers were purified by reversed-phase high-performance liquid chromatography (RP-HPLC) (Scheme 1). The successful syntheses were confirmed by matrix-assisted laser desorption ionization time-of-flight mass spectrometry (MALDI-TOF MS) (Figures S9–S12).

Polymerization of protDNA Macromonomers. Next, we carried out the homopolymerization of the protDNA macromonomers by ROMP in DCM using the third-generation Grubbs catalyst. The reaction was initiated at $-20\text{ }^{\circ}\text{C}$ for 5 min, transferred to an ice bath, and warmed to room temperature overnight. Following deprotection, the poly(oligonucleotide) products were examined by aqueous gel permeation chromatography (GPC) and gel electro-

phoresis (Figures 2, S1 and Table 1). All protDNA macromonomers were able to polymerize with polydispersity

Table 1. Aqueous GPC Analyses of Poly(Oligonucleotide) Bottlebrush Polymers from protDNA Macromonomers with Varying Monomer/Initiator Feed Ratios and Norbornene Position^a

entry	protDNA macromonomer structure (5'-3')	feed ratio	M_n (kDa)	DP_n	PDI	yield (%)
1	NB-(C12) ₂ -Her2-T*-Mal (5'-ODMT)	2:1	67.3	10.9	1.4	86
2	NB-(C12) ₂ -Her2-T*-Mal (5'-ODMT)	5:1	91.0	14.6	1.4	88
3	NB-(C12) ₂ -HER2-T*-Mal (5'-ODMT)	20:1	101.0	16.1	1.4	88
4	NB-(C12) ₂ -HER2-T*-Mal (5'-ODMT)	40:1				<5
5	NB-(C12) ₂ -HER2-T ^a -Mal (5'-OH)	2:1	77.0	12.7	1.2	63
6	NB-(C12) ₂ -HER2-T ^a -Mal (5'-OH)	5:1	86.5	14.5	1.4	67
7	NB-(C12) ₂ -HER2-T ^a -Mal (5'-OH)	20:1	121.0	20.3	1.3	36
8	NB-(C12) ₂ -HER2-T ^a -Mal (5'-OH)	40:1	169.8	28.5	1.1	20
9	HER2-(C12) ₂ -NB-T ^a -Mal (3'-T)	2:1	37.7	5.9	1.3	69
10	HER2-(C12) ₂ -NB-T ^a -Mal (3'-T)	5:1	35.8	5.7	1.5	61
11	HER2-(C12) ₂ -NB-T ^a -Mal (3'-T)	20:1	80.5	12.9	1.5	50
12	HER2-(C12) ₂ -NB-T ^a -Mal (3'-T)	40:1				<5
13	HER2-(C12) ₂ -NB-dS ^{aa} -Mal (3'-dS)	5:1	63.1	10.1	1.3	85
14	HER2-(C12) ₂ -NB-dS ^{aa} -Mal (3'-dS)	20:1	74.9	12.0	1.4	15

^a*3' nonphosphorylated macromonomer synthesized from "traceless" disulfide-linked CPG. **3' phosphorylated macromonomer synthesized from regular disulfide-linked CPG. For chemical structures, see Scheme S2 and Figure S7.

indices (PDIs) in the range of 1.10–1.65 (Table 1; the PDI is based on calibration with sodium polystyrene sulfonate, Scientific Polymer Products, Inc.). One observation is that, as the monomer/initiator feed ratio increases, reaction yield decreases, often significantly. In addition, the product molecular weight (MW) does not match the MW expected from feed stoichiometry. Rather, the measured number-average degree of polymerization (DP_n) is higher than that expected at low monomer/initiator ratios, but lower than that expected at high feed ratios. The seemingly uncontrolled polymerization characteristics can be explained by small amounts of contaminants in the reaction system poisoning a portion of the catalyst, which increases the effective monomer/initiator ratio. Indeed, the reactions were carried out at very small scales (5–20 nmol of catalysts in 10–20 μ L of solvent) because of limited availability of monomers, making the impact from contaminants much more evident. Additional work is needed to determine the identity of the contaminants. At the high feed ratios, the MW likely becomes limited by the sterics of the propagating chain end and/or product solubility in DCM, with a maximum DP_n of \sim 28.

The steric effect plays an important role in the polymerization of macromonomers.³⁶ Therefore, given the large size of protDNA, spacers may be necessary between the norbornene

group and the rest of the macromonomer. To test the impact of steric hindrance, 5' norbornene macromonomers with one or two dodecyl spacers (C12) were synthesized, which gave polymerization yields of 65 and 85%, respectively, at a fixed feed ratio of 20:1 (Table S1). These results indicate that the steric hindrance can be partially alleviated by elongating the spacer length, and at least two C12 spacers are required to achieve a reasonable polymerization yield. It is typical for the hydrophobic DMT group to remain attached to the 5' OH of the oligonucleotide after solid-phase synthesis to facilitate purification. The group can be manually removed via a mild acidic detritylation solution (3% trichloroacetic acid in DCM or acetic acid) after purification is completed. In the above polymerization example, the bulky DMT group is 16 atoms away from the norbornene group. To test if the bulky DMT group hinders polymerization, the detritylated 5'-norbornene macromonomer (denoted as 5'-OH) was prepared and polymerized. The maximum DP_n obtainable was 28.5, compared to 16.1 for the DMT-on macromonomers (denoted as 5'-ODMT), providing supporting evidence that the steric hindrance near the norbornene group can limit the degree of polymerization (Figure 2, Table 1, entries 3 and 8). However, the yields are depressed with the DMT-off monomers, possibly because of the incomplete purification of macromonomers without the hydrophobic DMT group, causing an increase in catalyst-damaging reactions. Accordingly, we speculate that the upper limit of DP may increase as the reaction is carried out in larger scales. A similar result was observed for 3'-norbornene macromonomers (denoted as 3'-T). Because of the use of "traceless" CPG as the solid support, the norbornene modifier is added after the first thymidine nucleotide, placing the two groups in close proximity which may cause steric interference (Figure 2). As a result, the DP_n values at all tested feed ratios (Table 1, entries 9–12) are lower compared with that of 5'-norbornene macromonomers, with or without the DMT group.

Polymerization of protDNA-*b*-PEG Macromonomers.

PEG has been widely adopted in pharmaceutical research and industry to improve biologics' pharmacological characteristics^{37,38} such as pharmacokinetics^{39,40} and tissue retention.⁴¹ Notwithstanding, the PEGylation of oligonucleotides using conventional linear or slightly branched PEG has not been able to provide sufficient steric protection, resulting in limited commercial success in drug formulation compared with other forms of PEGylated biologics (e.g., peptides and proteins).^{19,42,43} We have recently developed a class of bottlebrush-type PEGylated oligonucleotide conjugates (termed polymer-assisted compaction of DNA, or pacDNA) with a small number of oligonucleotides tethered to the backbone of a PEG-grafted bottlebrush polymer.^{19,20,44,45} Notably, these highly branched and densely arranged PEG side chains create a more compact PEG environment that can effectively shield oligonucleotides from interactions with proteins, which diminishes enzymatic degradation and alleviates side effects stemming from those interactions such as unwanted immune system activation and coagulopathy. Importantly, the dense PEGylation still allows for hybridization to the complementary target sequence with near-identical binding kinetics and thermodynamics.⁴⁶ We speculate that the DNA macromonomer approach can provide access to structural analogues of prototypical pacDNAs using protDNA-*b*-PEG block copolymers as the macromonomer, which simultaneously increases the oligonucleotide loading density.

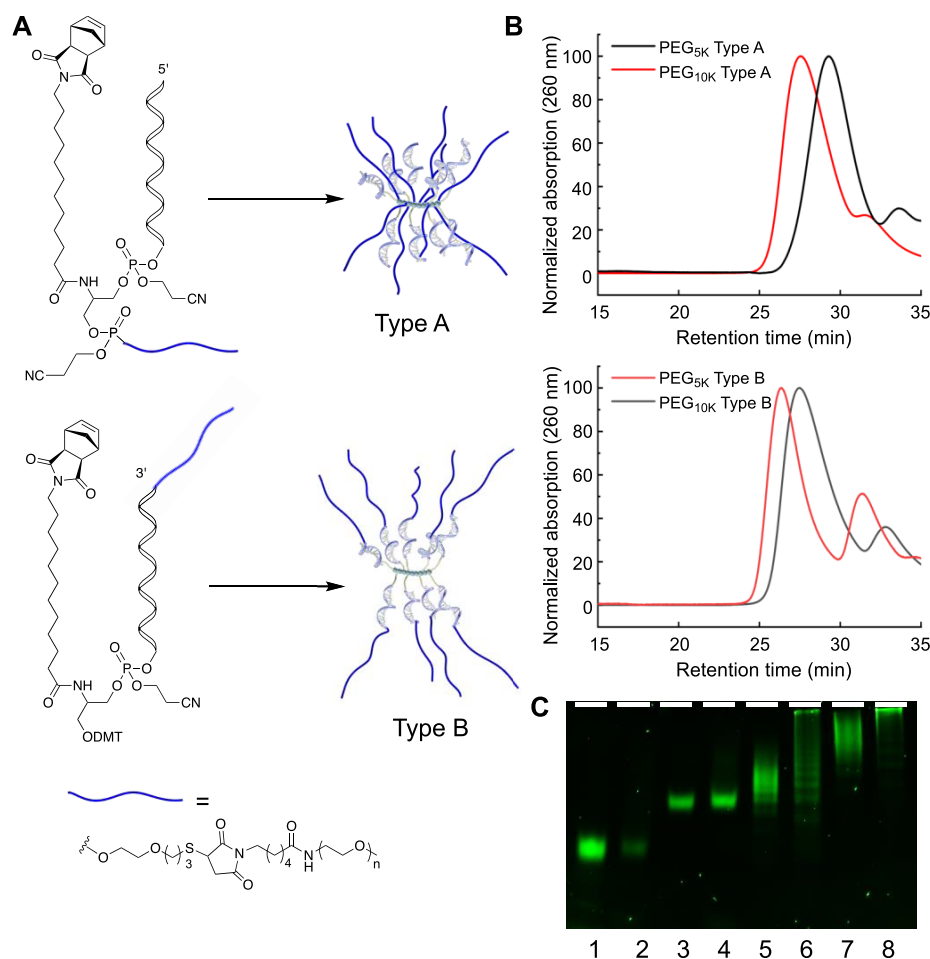


Figure 3. (A) Structures of protDNA-*b*-PEG macromonomers and the corresponding bottlebrush polymers. (B) Representative aqueous GPC chromatograms of Type A and B bottlebrush polymers from DNA-*b*-PEG_{5k}/PEG_{10k} macromonomers polymerized at a monomer/initiator ratio of 5:1. (C) Representative PAGE (4–20%) of DNA-*b*-PEG_{5k}/PEG_{10k} macromonomers and corresponding bottlebrush polymers polymerized at a monomer/initiator ratio of 5:1 (deprotected). Lanes: (1) Type A PEG_{5k} macromonomer, (2) Type B PEG_{5k} macromonomer, (3) Type A PEG_{10k} macromonomer, (4) Type B PEG_{10k} macromonomer, (5) Type A PEG_{5k} bottlebrush polymer, (6) Type B PEG_{5k} bottlebrush polymer, (7) Type A PEG_{10k} bottlebrush polymer, (8) Type B PEG_{10k} bottlebrush polymer. White bar represents loading well.

In addition, this modular design allows for greater freedom with regard to the positioning of the norbornene group, which should lead to architecturally diverse bottlebrush copolymers. Thus, we designed two protDNA-*b*-PEG macromonomers, where the norbornene group is placed either at the juncture of the two blocks (3' of the DNA), or at the distal end of the macromonomer (5' of the DNA). These macromonomers should result in two distinct types of PEGylated oligonucleotides (Figure 1): the former will result in the PEG chains being attached near the bottlebrush backbone (Type A), and the latter will have PEG chains tethered to the outer periphery of the DNA side chains (Type B).

To synthesize the diblock macromonomers, the protDNA was first prepared using norbornene phosphoramidite. After the cleavage, the exposed 3' sulfhydryl group provides a conjugation site that allows for the attachment of maleimide-modified PEG ($M_w = 5, 10$ kDa) (Scheme 1). Quantitative PEGylation can be accomplished using an excess of PEG (4–5 equivalent maleimide: sulfhydryl in the water/acetonitrile, $v/v = 1:1$) at 4 °C for 24 h. Unreacted PEG was removed via RP-HPLC, and successful synthesis of the conjugates was confirmed by MALDI-TOF MS and gel electrophoresis (Figures S6, S13–S19). Macromonomers for both types of

bottlebrushes can be synthesized in the same fashion independent of the position of the norbornene group (3' or 5').

Next, we carried out polymerizations using the diblock macromonomers, and the resulting bottlebrush polymers were characterized using aqueous GPC and gel electrophoresis (Figure 3 and Table 2). Considering that PEGylation substantially improves the solubility of protDNA in DCM, we first examined the impact of monomer concentration on polymerization, because a higher monomer concentration can often promote polymerization and counteract entropic factors from a thermodynamic perspective.⁴⁷ The Type A macromonomer with 5 kDa PEG was dissolved in DCM at two concentrations: 0.18 mM (the approximate upper solubility limit of non-PEG-modified macromonomer) and 1.80 mM. Upon polymerization under otherwise identical conditions with a feed ratio of 5:1, the monomer conversions were 74 and 90%, respectively, which are in line with expectations (Table 2, entries 1 and 2). Subsequent polymerizations were carried out with 1.80 mM macromonomers. When increasing the monomer/initiator ratio from 5:1 to 20:1, the DP_n plateaus at approximately 8–10, yet the polymerization yield drops drastically, from ~80 to <5%. The DP and yield for the

Table 2. Aqueous GPC Analyses of Type A and Type B Bottlebrush Polymers from protDNA-*b*-PEG Macromonomers with Varying Monomer/Initiator Feed Ratios, Norbornene Positions, and PEG Sizes

entry	protDNA- <i>b</i> -PEG macromonomer (5'-3')	Type	feed ratio	M_n (kDa)	DP_n	PDI	yield (%)
1	HER2-(C12) ₂ -NB-Mal-PEG _{5k}	A	5:1 ^a	84.8	7.5	1.2	74
2	HER2-(C12) ₃ -NB-Mal-PEG _{5k}	A	5:1	81.1	7.2	1.2	95
3	HER2-(C12) ₂ -NB-Mal-PEG _{5k}	A	10:1	66.4	5.9	1.2	26
4	HER2-(C12) ₂ -NB-Mal-PEG _{5k}	A	20:1				<5
5	HER2-(C12) ₃ -NB-Mal-PEG _{5k}	A	2:1	58.0	5.2	1.3	90
6	HER2-(C12) ₃ -NB-Mal-PEG _{5k}	A	5:1	83.1	7.2	1.2	80
7	HER2-(C12) ₃ -NB-Mal-PEG _{5k}	A	10:1	85.6	7.4	1.2	38
8	HER2-(C12) ₂ -NB-Mal-PEG _{10k}	A	5:1	135.9	8.2	1.1	61
9	HER2-(C12) ₂ -NB-Mal-PEG _{10k}	A	10:1				<5
10	HER2-(C12) ₃ -NB-Mal-PEG _{10k}	A	2:1	86.4	5.2	1.4	87
11	HER2-(C12) ₃ -NB-Mal-PEG _{10k}	A	5:1	140.2	8.4	1.2	85
12	HER2-(C12) ₃ -NB-Mal-PEG _{10k}	A	10:1	160.0	9.6	1.1	60
13	HER2-(C12) ₃ -NB-Mal-PEG _{10k}	A	20:1				<5
14	NB-(C12) ₂ -HER2-Mal-PEG _{5k}	B	5:1	130.5	11.5	1.2	83
15	NB-(C12) ₂ -HER2-Mal-PEG _{5k}	B	10:1	160.9	14.2	1.2	95
16	NB-(C12) ₂ -HER2-Mal-PEG _{10k}	B	5:1	160.3	9.5	1.1	63
17	NB-(C12) ₂ -HER2-Mal-PEG _{10k}	B	10:1	184.2	10.9	1.1	30

^aMonomer concentration is 0.18 mM.

polymerization of Type A macromonomers were slightly improved when an additional C12 spacer (for a total of three) was incorporated (Table 2, entries 3, 7, 9, and 12). We attribute the decrease in reaction yield and DP_n to the steric effect from the PEG. Interestingly, the PEG size (5 and 10 kDa) had no significant effect on the polymerization. It appears that the steric effect is more apparent with Type A macromonomers than with Type B macromonomers, likely because the PEG component is closer to the norbornene group for Type A macromonomers. For the two-spacer macromonomers, the Type B macromonomer with 5 kDa PEG achieved significantly improved DP_n (14.2 vs 5.9 at 10:1 feed ratio) and conversion (95 vs 26%). Similar results were observed with 10 kDa PEG. Dynamic light scattering (DLS) shows that the polymer hydrodynamic diameter is a function of PEG length and backbone DP_n and is generally within 8–20 nm (Table 3). ζ potential measurements have shown a “shielding” effect of the DNA surface charge by the grafted PEG,⁴⁸ with the average values of the bottlebrush in the range of –3.2 to –12.4 mV (–35 mV for the free DNA).

Table 3. DLS Size, ζ Potential, and Duplex Melting Temperature of the Type A and Type B Bottlebrush Polymers

	free DNA	Type A		Type B	
		PEG _{5k}	PEG _{10k}	PEG _{5k}	PEG _{10k}
number-average diameter (nm)	N.A.	7.9 ± 3.3	17.0 ± 2.6	11.1 ± 2.5	20.8 ± 4.3
ζ potential (mV)	–34.5 ± 0.8	–12.4 ± 1.0	–4.6 ± 1.3	–6.7 ± 3.1	–3.2 ± 1.4
duplex T_m (°C)	56.2 ± 1.4	58.6 ± 1.5	58.6 ± 1.5	61.6 ± 0.5	61.2 ± 0.3

To further investigate whether the hybridization kinetics of oligonucleotides were influenced by the presence of the side chain PEG, PEG size, and polymer architecture, a fluorescence quenching assay was adopted.^{21,49} A quencher (dabcyl)-modified strand was used to hybridize with fluorescein-labeled oligonucleotides in the bottlebrush polymer. Hybridization and thermal melting result in decreases and increases in fluorescence intensity, respectively. It was found that all the bottlebrush polymers, regardless of the PEG size and conjugation site, exhibited similar, near-instantaneous hybridization kinetics as the free DNA (Figure S2). This result indicates that the local PEG densities of the bottlebrush copolymers are not overly crowded that access to the conjugated oligonucleotide by a complementary strand is blocked, which is consistent with our previous findings with pacDNAs. To examine the inhibition of protein access, pre-hybridized free oligonucleotide and bottlebrush copolymer duplexes were treated with DNase I (an endonuclease that nonspecifically and predominantly cleaves double-stranded DNA). Upon degradation, the fluorophore quencher pair is separated, leading to an increase of fluorescence signal (Figure S2). Both Type A and Type B exhibited slightly enhanced nuclease resistance with as much as twofold increase in enzymatic half-life compared to free DNA, suggesting that the PEG density created by the bottlebrush architecture is able to provide steric selectivity to the oligonucleotides. However, interestingly, Type B bottlebrushes appear to exhibit slightly greater enzymatic resistance. Thus, although the PEG component in Type B bottlebrushes is located further away from the polymer backbone, creating a lower PEG density overall, the fact that the oligonucleotides reside within a PEG corona is able to counteract the reduced PEG density. Future designs involving a Y-shaped PEG tethered to the terminus of oligonucleotide macromonomers may be able to yield bottlebrushes with even greater steric selectivity. Interestingly, both types of bottlebrushes exhibit increased melting temperature (T_m) compared to free DNA. This observation may be attributed to the volume exclusion effect of neighboring macromolecules (PEG) on double-stranded DNA (dsDNA). In addition, an increase in local salt concentration due to a dense arrangement of oligonucleotides is known to increase the T_m of dsDNA. In particular, the Type B bottlebrush shows a higher T_m than Type A (~61 vs 59 °C), independent of PEG size (Figure S3, Table 3). The lower T_m for Type A bottlebrush compared to Type B can be explained by the destabilizing effect induced by the PEG through favorable preferential interactions with the nucleotide base surface, which is similar to effects induced by low-MW PEG in a cosolute system.^{50,51} Type A bottlebrush is architecturally set up for more of the preferential interaction compared to Type B.

CONCLUSIONS

In conclusion, we have expanded the toolbox for poly-(oligonucleotide)-type materials by introducing a norbornene phosphoramidite, which allows for the direct incorporation of a polymerizable group into a desired position of the oligonucleotide sequence. Steric hindrance has been identified as a limiting factor to attain high-molecular-weight bottlebrushes. We demonstrate that poly(oligonucleotide) structures with varying conjugation sites and copolymer architectures are possible. Two distinct types of PEG-modified bottlebrushes with PEG containing side chains were synthesized. We found that when the PEG is tethered to the termini of the oligonucleotide, steric selectivity is slightly greater than when it is tethered near the polymer backbone. We envision that, with expanding access to DNA-polymer conjugates of more complex architectures, the discovery of novel properties and applications of these materials will follow shortly.

ASSOCIATED CONTENT

Supporting Information

The Supporting Information is available free of charge at <https://pubs.acs.org/doi/10.1021/acs.macromol.1c02624>.

Experimental procedures and additional characterization data (PDF)

AUTHOR INFORMATION

Corresponding Author

Ke Zhang – Departments of Chemistry and Chemical Biology, Bioengineering, and Chemical Engineering, Northeastern University, Boston, Massachusetts 02115, United States; orcid.org/0000-0002-8142-6702; Email: k.zhang@northeastern.edu

Authors

Hao Lu – Departments of Chemistry and Chemical Biology, Bioengineering, and Chemical Engineering, Northeastern University, Boston, Massachusetts 02115, United States

Jiansong Cai – Departments of Chemistry and Chemical Biology, Bioengineering, and Chemical Engineering, Northeastern University, Boston, Massachusetts 02115, United States

Yang Fang – Departments of Chemistry and Chemical Biology, Bioengineering, and Chemical Engineering, Northeastern University, Boston, Massachusetts 02115, United States

Mengqi Ren – Departments of Chemistry and Chemical Biology, Bioengineering, and Chemical Engineering, Northeastern University, Boston, Massachusetts 02115, United States

Xuyu Tan – Department of Chemistry, Massachusetts Institute of Technology, Cambridge, Massachusetts 02139, United States

Fei Jia – Department of Chemistry, Massachusetts Institute of Technology, Cambridge, Massachusetts 02139, United States

Dali Wang – Departments of Chemistry and Chemical Biology, Bioengineering, and Chemical Engineering, Northeastern University, Boston, Massachusetts 02115, United States

Complete contact information is available at:

<https://pubs.acs.org/doi/10.1021/acs.macromol.1c02624>

Author Contributions

[§]H.L. and J.C. contributed equally.

Author Contributions

The manuscript was written through contributions of all authors. All authors have given approval to the final version of the manuscript.

Funding

Research reported in this publication was supported by the National Science Foundation (DMR award number 2004947), National Institute of General Medical Sciences (1R01GM121612), and National Cancer Institute (1R01CA251730).

Notes

The authors declare no competing financial interest.

ACKNOWLEDGMENTS

The authors thank Dr. Roman Manetsch for assistance with LC-MS.

REFERENCES

- (1) Kulkarni, J. A.; Witzigmann, D.; Thomson, S. B.; Chen, S.; Leavitt, B. R.; Cullis, P. R.; van der Meel, R. The current landscape of nucleic acid therapeutics. *Nat. Nanotechnol.* **2021**, *16*, 630–643.
- (2) Kim, J.; Hu, C.; Moufawad El Achkar, C.; Black, L. E.; Douville, J.; Larson, A.; Pendergast, M. K.; Goldkind, S. F.; Lee, E. A.; Kuniholm, A.; Soucy, A.; Vaze, J.; Belur, N. R.; Fredriksen, K.; Stojkowska, I.; Tsytsykova, A.; Armant, M.; DiDonato, R. L.; Choi, J.; Cornelissen, L.; Pereira, L. M.; Augustine, E. F.; Genetti, C. A.; Dies, K.; Barton, B.; Williams, L.; Goodlett, B. D.; Riley, B. L.; Pasternak, A.; Berry, E. R.; Pflock, K. A.; Chu, S.; Reed, C.; Tyndall, K.; Agrawal, P. B.; Beggs, A. H.; Grant, P. E.; Urion, D. K.; Snyder, R. O.; Waisbren, S. E.; Poduri, A.; Park, P. J.; Patterson, A.; Biffi, A.; Mazzulli, J. R.; Bodamer, O.; Berde, C. B.; Yu, T. W. Patient-Customized Oligonucleotide Therapy for a Rare Genetic Disease. *N. Engl. J. Med.* **2019**, *381*, 1644–1652.
- (3) Roberts, T. C.; Langer, R.; Wood, M. J. A. Advances in oligonucleotide drug delivery. *Nat. Rev. Drug Discovery* **2020**, *19*, 673–694.
- (4) Xiong, H.; Veedu, R. N.; Diermeier, S. D. Recent Advances in Oligonucleotide Therapeutics in Oncology. *Int. J. Mol. Sci.* **2021**, *22*, 3295.
- (5) Efimov, V. A.; Buryakova, A. A.; Chakhmakhcheva, O. G. Synthesis of polyacrylamides N-substituted with PNA-like oligonucleotide mimics for molecular diagnostic applications. *Nucleic Acids Res.* **1999**, *27*, 4416–4426.
- (6) Roth Stina, B.; Jalava, J.; Ruuskanen, O.; Ruohola, A.; Nikkari, S. Use of an Oligonucleotide Array for Laboratory Diagnosis of Bacteria Responsible for Acute Upper Respiratory Infections. *J. Clin. Microbiol.* **2004**, *42*, 4268–4274.
- (7) Tavitian, B. In vivo imaging with oligonucleotides for diagnosis and drug development. *Gut* **2003**, *52*, iv40.
- (8) Carter, L. J.; Garner, L. V.; Smoot, J. W.; Li, Y.; Zhou, Q.; Saveson, C. J.; Sasso, J. M.; Gregg, A. C.; Soares, D. J.; Beskid, T. R.; Jervey, S. R.; Liu, C. Assay Techniques and Test Development for COVID-19 Diagnosis. *ACS Cent. Sci.* **2020**, *6*, 591–605.
- (9) Storici, F.; Lewis, L. K.; Resnick, M. A. In vivo site-directed mutagenesis using oligonucleotides. *Nat. Biotechnol.* **2001**, *19*, 773–776.
- (10) Li, G.; Zheng, W.; Chen, Z.; Zhou, Y.; Liu, Y.; Yang, J.; Huang, Y.; Li, X. Design, preparation, and selection of DNA-encoded dynamic libraries. *Chem. Sci.* **2015**, *6*, 7097–7104.
- (11) Seeman, N. C. Structural DNA nanotechnology: an overview. *Methods Mol. Biol.* **2005**, *303*, 143–166.
- (12) Seeman, N. C. The design and engineering of nucleic acid nanoscale assemblies. *Curr. Opin. Struct. Biol.* **1996**, *6*, 519–526.
- (13) He, L.; Lu, D.; Liang, H.; Xie, S.; Zhang, X.; Liu, Q.; Yuan, Q.; Tan, W. mRNA-Initiated, Three-Dimensional DNA Amplifier Able to Function inside Living Cells. *J. Am. Chem. Soc.* **2018**, *140*, 258–263.

- (14) Huang, H.; Guo, Z.; Zhang, C.; Cui, C.; Fu, T.; Liu, Q.; Tan, W. Logic-Gated Cell-Derived Nanovesicles via DNA-Based Smart Recognition Module. *ACS Appl. Mater. Interfaces* **2021**, *13*, 30397–30403.
- (15) Tan, X.; Li, B. B.; Lu, X.; Jia, F.; Santori, C.; Menon, P.; Li, H.; Zhang, B.; Zhao, J. J.; Zhang, K. Light-Triggered, Self-Immolative Nucleic Acid-Drug Nanostructures. *J. Am. Chem. Soc.* **2015**, *137*, 6112–6115.
- (16) Zhao, N.; Pei, S.-N.; Qi, J.; Zeng, Z.; Iyer, S. P.; Lin, P.; Tung, C.-H.; Zu, Y. Oligonucleotide aptamer-drug conjugates for targeted therapy of acute myeloid leukemia. *Biomaterials* **2015**, *67*, 42–51.
- (17) Fang, Y.; Lu, X.; Wang, D.; Cai, J.; Wang, Y.; Chen, P.; Ren, M.; Lu, H.; Union, J.; Zhang, L.; Sun, Y.; Jia, F.; Kang, X.; Tan, X.; Zhang, K. Spherical Nucleic Acids for Topical Treatment of Hyperpigmentation. *J. Am. Chem. Soc.* **2021**, *143*, 1296–1300.
- (18) Banga, R. J.; Krovi, S. A.; Narayan, S. P.; Sprangers, A. J.; Liu, G. L.; Mirkin, C. A.; Nguyen, S. T. Drug-Loaded Polymeric Spherical Nucleic Acids: Enhancing Colloidal Stability and Cellular Uptake of Polymeric Nanoparticles through DNA Surface-Functionalization. *Biomacromolecules* **2017**, *18*, 483–489.
- (19) Lu, X. G.; Zhang, K. PEGylation of therapeutic oligonucleotides: From linear to highly branched PEG architectures. *Nano Res.* **2018**, *11*, 5519–5534.
- (20) Jia, F.; Lu, X.; Wang, D.; Cao, X.; Tan, X.; Lu, H.; Zhang, K. Depth-Profiling the Nuclease Stability and the Gene Silencing Efficacy of Brush-Architected Poly(ethylene glycol)–DNA Conjugates. *J. Am. Chem. Soc.* **2017**, *139*, 10605–10608.
- (21) Cutler, J. I.; Auyeung, E.; Mirkin, C. A. Spherical Nucleic Acids. *J. Am. Chem. Soc.* **2012**, *134*, 1376–1391.
- (22) Tan, X.; Lu, H.; Sun, Y.; Chen, X.; Wang, D.; Jia, F.; Zhang, K. Expanding the Materials Space of DNA via Organic-Phase Ring-Opening Metathesis Polymerization. *Chem* **2019**, *5*, 1584–1596.
- (23) Winkler, J. Oligonucleotide conjugates for therapeutic applications. *Ther. Delivery* **2013**, *4*, 791–809.
- (24) Kwak, M.; Herrmann, A. Nucleic acid amphiphiles: synthesis and self-assembled nanostructures. *Chem. Soc. Rev.* **2011**, *40*, 5745–5755.
- (25) Hurst, S. J.; Lytton-Jean, A. K. R.; Mirkin, C. A. Maximizing DNA Loading on a Range of Gold Nanoparticle Sizes. *Anal. Chem.* **2006**, *78*, 8313–8318.
- (26) Liu, B.; Liu, J. Methods for preparing DNA-functionalized gold nanoparticles, a key reagent of bioanalytical chemistry. *Anal. Methods* **2017**, *9*, 2633–2643.
- (27) Sun, D.; Gang, O. DNA-Functionalized Quantum Dots: Fabrication, Structural, and Physicochemical Properties. *Langmuir* **2013**, *29*, 7038–7046.
- (28) Nakano, S.-I.; Sugimoto, N. The structural stability and catalytic activity of DNA and RNA oligonucleotides in the presence of organic solvents. *Biophys. Rev.* **2016**, *8*, 11–23.
- (29) Mel'nikov, S. M.; Khan, M. O.; Lindman, B.; Jönsson, B. Phase Behavior of Single DNA in Mixed Solvents. *J. Am. Chem. Soc.* **1999**, *121*, 1130–1136.
- (30) Dizdaroglu, M. Oxidatively induced DNA damage: Mechanisms, repair and disease. *Cancer Lett.* **2012**, *327*, 26–47.
- (31) Angelé-Martínez, C.; Goodman, C.; Brumaghim, J. Metal-mediated DNA damage and cell death: mechanisms, detection methods, and cellular consequences. *Metallomics* **2014**, *6*, 1358–1381.
- (32) James, C. R.; Rush, A. M.; Insley, T.; Vukovic, L.; Adamiak, L.; Kral, P.; Gianneschi, N. C. Poly(oligonucleotide). *J. Am. Chem. Soc.* **2014**, *136*, 11216–11219.
- (33) Liu, K.; Zheng, L. F.; Liu, Q.; de Vries, J. W.; Gerasimov, J. Y.; Herrmann, A. Nucleic Acid Chemistry in the Organic Phase: From Functionalized Oligonucleotides to DNA Side Chain Polymers. *J. Am. Chem. Soc.* **2014**, *136*, 14255–14262.
- (34) Arkinstall, L. A.; Husband, J. T.; Wilks, T. R.; Foster, J. C.; O'Reilly, R. K. DNA-polymer conjugates via the graft-through polymerisation of native DNA in water. *Chem. Commun.* **2021**, *57*, 5466–5469.
- (35) de Rochambeau, D.; Sun, Y. Y.; Barlog, M.; Bazzi, H. S.; Sleiman, H. F. Modular Strategy To Expand the Chemical Diversity of DNA and Sequence-Controlled Polymers. *J. Org. Chem.* **2018**, *83*, 9774–9786.
- (36) Ren, N.; Yu, C. Y.; Zhu, X. Y. Topological Effect on Macromonomer Polymerization. *Macromolecules* **2021**, *54*, 6101–6108.
- (37) Thakur, S.; Kesharwani, P.; Tekade, R. K.; Jain, N. K. Impact of pegylation on biopharmaceutical properties of dendrimers. *Polymer* **2015**, *59*, 67–92.
- (38) Turecek, P. L.; Bossard, M. J.; Schoetens, F.; Ivens, I. A. PEGylation of Biopharmaceuticals: A Review of Chemistry and Nonclinical Safety Information of Approved Drugs. *J. Pharm. Sci.* **2016**, *105*, 460–475.
- (39) Veronese, F. M.; Pasut, G. PEGylation, successful approach to drug delivery. *Drug Discovery Today* **2005**, *10*, 1451–1458.
- (40) Wang, J. Q.; Mao, W. W.; Lock, L. L.; Tang, J. B.; Sui, M. H.; Sun, W. L.; Cui, H. G.; Xu, D.; Shen, Y. Q. The Role of Micelle Size in Tumor Accumulation, Penetration, and Treatment. *ACS Nano* **2015**, *9*, 7195–7206.
- (41) Suk, J. S.; Xu, Q. G.; Kim, N.; Hanes, J.; Ensign, L. M. PEGylation as a strategy for improving nanoparticle-based drug and gene delivery. *Adv. Drug Delivery Rev.* **2016**, *99*, 28–51.
- (42) Alconcel, S. N. S.; Baas, A. S.; Maynard, H. D. FDA-approved poly(ethylene glycol)-protein conjugate drugs. *Polym. Chem.* **2011**, *2*, 1442–1448.
- (43) Kolate, A.; Baradia, D.; Patil, S.; Vhora, I.; Kore, G.; Misra, A. PEG — A versatile conjugating ligand for drugs and drug delivery systems. *J. Controlled Release* **2014**, *192*, 67–81.
- (44) Wang, D. L.; Lin, J. Q.; Jia, F.; Tan, X. Y.; Wang, Y. Y.; Sun, X. Y.; Cao, X. Y.; Che, F. Y.; Lu, H.; Gao, X. M.; Shimkonis, J. C.; Nyoni, Z.; Lu, X. G.; Zhang, K. Bottlebrush-architected poly(ethylene glycol) as an efficient vector for RNA interference in vivo. *Sci. Adv.* **2019**, *5*, No. eaav9322.
- (45) Cao, X. Y.; Lu, X. G.; Wang, D. L.; Jia, F.; Tan, X. Y.; Corley, M.; Chen, X. Y.; Zhang, K. Modulating the Cellular Immune Response of Oligonucleotides by Brush Polymer-Assisted Compaction. *Small* **2017**, *13*, No. 1701432.
- (46) Jia, F.; Lu, X. G.; Tan, X. Y.; Wang, D. L.; Cao, X. Y.; Zhang, K. Effect of PEG Architecture on the Hybridization Thermodynamics and Protein Accessibility of PEGylated Oligonucleotides. *Angew. Chem., Int. Ed.* **2017**, *56*, 1239–1243.
- (47) Pearce, A. K.; Foster, J. C.; O'Reilly, R. K. Recent developments in entropy-driven ring-opening metathesis polymerization: Mechanistic considerations, unique functionality, and sequence control. *J. Polym. Sci., Part A: Polym. Chem.* **2019**, *57*, 1621–1634.
- (48) Kumar, V.; Qin, J.; Jiang, Y. F.; Duncan, R. G.; Brigham, B.; Fishman, S.; Nair, J. K.; Akinc, A.; Barros, S. A.; Kasperkovitz, P. V. Shielding of Lipid Nanoparticles for siRNA Delivery: Impact on Physicochemical Properties, Cytokine Induction, and Efficacy. *Mol. Ther.—Nucleic Acids* **2014**, *3*, e210.
- (49) Randeria, P. S.; Jones, M. R.; Kohlstedt, K. L.; Banga, R. J.; de la Cruz, M. O.; Schatz, G. C.; Mirkin, C. A. What Controls the Hybridization Thermodynamics of Spherical Nucleic Acids? *J. Am. Chem. Soc.* **2015**, *137*, 3486–3489.
- (50) Knowles, D. B.; LaCroix, A. S.; Deines, N. F.; Shkel, I.; Record, M. T. Separation of preferential interaction and excluded volume effects on DNA duplex and hairpin stability. *Proc. Natl. Acad. Sci. U. S. A.* **2011**, *108*, 12699–12704.
- (51) Guin, D.; Gruebele, M. Weak Chemical Interactions That Drive Protein Evolution: Crowding, Sticking, and Quinary Structure in Folding and Function. *Chem. Rev.* **2019**, *119*, 10691–10717.